18th International Conference on Structural Mechanics in Reactor Technology (SMiRT 18)
Beijing, China, August 7-12, 2005
SMiRT18-D07-1

LIFE-TIME PREDICTION OF AUSTENITIC STAINLESS STEEL BY APPLYING MAGNETIC NDT-METHODS

Markus Niffenegger*
PAUL SCHERRER INSTITUT
Nuclear Energy and Safety Department
CH-5232 Villigen PSI, Switzerland
Phone: +41 563102686, Fax:+41 563102199
E-mail: Markus.Niffenegger@psi.ch

Hans J. Leber
PAUL SCHERRER INSTITUT
Nuclear Energy and Safety Department
CH-5232 Villigen PSI, Switzerland

Dietmar Kalkhof
PAUL SCHERRER INSTITUT
Nuclear Energy and Safety Department
CH-5232 Villigen PSI, Switzerland

ABSTRACT

The detection of material degradation prior to technical crack initiation of safety-relevant components, like piping in the primary circuit of nuclear power plants, is an ongoing research topic. Since in some metastable austenitic stainless steels (paramagnetic), fatigue is accompanied by a transformation of the face centred cubic phase (γ-fcc) into the body centred cubic martensitic (ferromagnetic) phase (α'-bcc) with a slight distortion to a tetragonal shape, the corresponding changes of magnetic properties can be used as an indication for the remaining life time of in-service components. However, the affinity for such phase transitions depends on several parameters e.g. temperature, chemical composition of the material, heat treatment, state of cold working and loading conditions. These influencing parameters have to be analysed carefully in order to allow a reliable prediction of the remaining operation-time of safety relevant components.

In this paper we compare different methods for the detection of martensitic contents concerning their performance and potential for the application in laboratory and plant environment. These are: quantitative evaluation of martensite by neutron diffraction as a calibration method, measurement of the eddy current impedance by means of giant magneto-resistance sensors (GMR), magnetic remanence field measurement by fluxgate sensors and the determination of magnetic permeability using a Ferromaster®. Furthermore, the influence of the chemical composition, heat treatment, operation temperature and applied load on the affinity for martensitic transformations is discussed.

It is shown, that all the investigated magnetic measuring methods are able to detect the amount of martensite in fatigue specimens. However, their application requires the knowledge of material specific calibration curves and is limited by the low affinity for martensitic transformation of some austenitic stainless steels.

The results presented in this paper contribute to failure analyses of austenitic stainless steel components. For fatigue relevant components, an increase of the martensitic phase content is an indication for a certain accumulated plastic deformation. A screening criterion for the volume fraction of martensite for the given material and loading conditions can be used to avoid technical cracks caused by thermo-mechanical fatigue.

Keywords: Material degradation, austenitic stainless steel, martensite, neutron diffraction, magnetic non-destructive material testing, lifetime prediction, low cycle fatigue.

1. INTRODUCTION

Lifetime extension of in-service nuclear power plants (NPP) is an economical way to reduce costs for the generation of electricity and therefore has become of major interest in the last few years. Furthermore, the prevention of crack growth, mainly caused by thermal fatigue, as already appeared e.g. in a pipe of the Civaux NPP, is an important demand.

To qualify nuclear components for lifetime extension in a safe manner, corresponding inspections of safety relevant components are therefore required. Existing "state of the art techniques" for in-service inspection are mainly specialized for crack detection. However, the detection of material degradation in a pre-cracked stage would be very advantageous, but this requires the development of innovative reliable non-destructive testing (NDT) methods for the inspection of critical components. The aim of such methods is to detect micro-structural material changes and finally to avoid undesired events, e.g. caused by changing operation parameters, decreasing inspection intervals or replacement of expensive components.

The main objective of this paper is the assessment of the capability and reliability of some magnetic NDT-techniques. These techniques are sensitive to micro-structural changes, which may change the mechanical properties of a component long before macroscopic cracks are initiated and eventually grow. However, these indirect methods described below also require a careful interpretation of the measured signal in terms of micro-structural evolutions of the material due to fatigue. Such microscopic analysis were also performed within the ongoing research and described in [1] and [2].

The ageing mechanism under investigation is thermo-mechanical fatigue (TMF) that occurs in austenitic stainless steel pipes due to varying temperature gradients. Such temperature transients might be caused by slow temperature swirls at "dead" ends, stratification in horizontal piping and at nozzles as well as by high-cycle mixing due to leakage flows at valves and high-cycle mixing at tees.

The effect that allows the detection of material degradation due to TMF by means of magnetic methods is a partial phase transformation of the material. It is known that in some meta-stable austenitic stainless steels a phase transformation from austenitic face centred cubic (fcc) lattice (γ) into a body centred cubic (bcc) lattice having a slight tetragonal shape, the so-called martensite (α') takes place under the influence of quasi-static or cyclic strain loading [3]. This phenomenon is called strain-induced martensitic transformation.

Since the martensite is ferromagnetic, whereas the γ-phase is paramagnetic, this change of magnetic properties can serve as an indication for the material degradation. We therefore use magnetic sensors for the detection of magnetic changes in low cycle fatigue specimens (LCF). In our investigation the following magnetic sensor systems were used:

- FERROMASTER® and Ferritscope® for measuring the magnetic permeability,
- 3-D-FLUXGATE for measuring the magnetic remanence field,
- GMR (Giant Magneto-Resistant) for measuring the eddy current impedance.

Since these indirect methods need a calibration concerning the amount of martensite, neutron diffraction (ND) was applied to quantify the amount of strain-induced martensite in LCF-specimens.

LCF-specimens made from various heats and materials were tested in low cycle fatigue conditions at different temperatures. The results have shown that beside strain amplitude and temperature other influencing parameters for the susceptibility of martensitic transformation played a crucial role. The influence of the chemical compositions on the affinity to form α' can be estimated by the well-known Schaeffler diagram. Further influencing parameters are the state of cold working and the kind of heat treatment. Therefore these influences have been investigated on different initial material states of the austenitic stainless steel grade AISI 321, AISI 304L and AISI 347.

In order to characterize the material in its un-fatigued as well as in its fatigued state and to consider micro-structural changes related to fatigue damage the methods listed below were employed [1]:

- Metallographic investigations to determine shape and size of grains and martensite
- Inductive Coupled Plasma Emission Photometry (ICP-OES) was applied to inspected the chemical composition as well as combustion (C and S)
- Scanning electron microscopy (SEM) for observing cracks, slip bands, twins and dislocation networks
- Physical Properties Measuring System (PPMS) for measuring magnetization characteristics

- Neutron- and advanced X-ray diffraction methods for the quantitative determination of martensitic contents
- Transmission electron microscopy (TEM) for the observation of crystalline defects as dislocations and micro-twins

Differences between the investigated metastable austenitic stainless steels concerning their microstructure and affinity for martensitic transformation were observed [4]. However, in this paper we concentrate on the determination of martensitic contents by means of ND and magnetic methods. We further discuss the influencing parameters and their consequences for the application of the mentioned magnetic NDT-methods.

2. MATERIAL DEPENDENT AFFINITY FOR STRAIN-INDUCED MARTENSITE FORMATION

For our investigations austenitic stainless steels were chosen for its relevance in the nuclear power plant piping and because of the meta-stable properties of the austenitic phase. The material under investigation is either of titanium- or niobium-stabilized and non-stabilized austenitic stainless steel type. Among the quality assurance procedure that included tension tests to evaluate the mechanical properties and metallographic investigation of the microstructure we also analysed the chemical composition of the received product. For this purpose Inductive Coupled Plasma Emission Photometry (ICP-OES) and combustion (C and S) was applied. The results of this analysis are summarized in Tab 1. In Tab. 2 we also indicate the material type and its condition of delivery, which is classified as cold worked (CW) or solution annealed (SA) bars, plates or pipes. From the three delivery forms, the pipes are the most important ones because they were foreseen to serve as surge lines in a nuclear power plant (NPP). However, the bar and plate material allowed the detailed investigation of martensitic transformation due to higher affinity for austenite-martensite phase transformation and the extensive testing of the magnetic NDT-methods.
Polished cylindrical fatigue specimens (Fig. 1) were machined out of these products. We tested the specimens under low cycle fatigue (LCF) condition with a defined number of cyclic strain loads. From the cylindrical part of the specimen a gauge volume of length 20 mm and a diameter of 8 mm or 10 mm was analysed by the methods discussed in the following chapters.

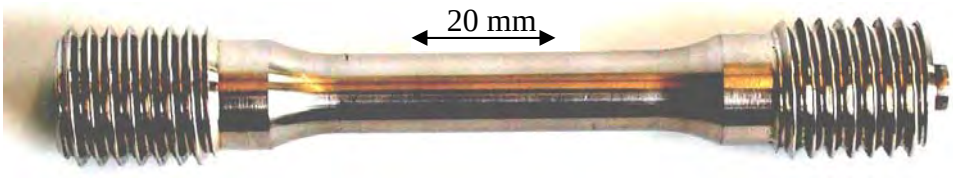

Fig. 1: Low cycle fatigue specimen. The cylindrical part was analysed.

Table 1: Chemical composition of analysed material (values in mass-%)

Product	C	Si	Mn	P	S	Cr	Mo	Ni	Co	Cu	N	Ti	Nb
Bar AISI 321	0.0332	0.43	1.87	0.030	0.025	17.8	0.351	9.92	0.121	0.363	0.024	0.146	0.002
Bar AISI 347	0.03	0.28	1.65	0.03	0.02	19.2	0.129	10.9	0.034	0.0594	0.014	0.0075	0.392
Plate AISI 321	0.0508	0.18	1.27	0.021	0.003	17.4	0.209	9.31	0.121	0.227	0.012	0.430	0.002
Plate AISI 304L	0.029	0.39	1.85	0.03	0.02	18.3	0.044	10.2	0.04	0.018	0.056	0.0013	0.001
Pipe AISI 321	0.07	0.20	1.87	0.021	0.004	18.0	0.334	10.2	0.055	0.182	0.010	0.517	0.0149
Pipe AISI 304L	0.0287	0.20	1.77	0.020	0.0036	19.0	0.122	10.35	0.0388	0.186		0.0020	0.0024
Pipe AISI 347	0.0554	0.27	1.74	0.023	0.0104	17.9	0.351	10.48	0.1018	0.225		0.00267	0.7165

Based on the chemical composition given in Tab.1 predictions concerning the martensite formation are possible. The position of the investigated steel products in the Schaeffler diagram (Fig. 2) allows an estimation of their affinity to martensite formation. For this purpose we calculate the chromium equivalent by (Eq. 1), taking into account the ferrite forming elements, and the nickel equivalent (Eq. 2), considering the austenite forming elements, according to the technical information by the steel supplier.

$$Cr_{eq} = 1.5Si + Cr + Mo + 2Ti + 0.5Nb \quad [\%] \qquad \text{(Eq. 1)}$$

$$Ni_{eq} = 30(C + N) + 0.5Mn + Ni + 0.5(Cu + Co) \quad [\%] \qquad \text{(Eq. 2)}$$

Table 2: Condition of delivery of the investigated products.
WQ to RT = water quenching to room temperature

Material	Processing	Final heat treatment
Bar, CW AISI 321	Solution annealed, cold worked (CW).	none
Bar, CW AISI 347	Solution annealed, cold worked (CW).	none
Plate, SA AISI 321	Hot rolled, solution annealed (SA).	1050 °C, WQ to RT
Plate, SA AISI 304L	Hot rolled, solution annealed (SA), cold worked (CW), solution annealed (SA) .	1050 °C, WQ to RT
Plate, CW AISI 304L	Hot rolled, solution annealed (SA), cold worked (CW).	none
Pipe, SA AISI 321	Tube rounds, forged, turned/belt ground; hot finished, solution annealed (SA).	1050 °C, WQ to RT
Pipe, SA AISI 304L	Tube rounds, forged, turned/belt ground; hot finished, solution annealed (SA).	1050 °C, WQ to RT
Pipe, SA AISI 347	Tube rounds, forged, turned/belt ground; hot finished, solution annealed (SA).	1050 °C, WQ to RT

Comparing the different material states we derive that the plate material AISI 321, which is found to be far in the two-phase region (austenite+martensite), has the highest susceptibility for martensitic transformation. A somewhat smaller affinity for α'-formation can be expected for AISI 347 pipe, AISI 321 bar and pipe material. Similarly, the position in the Schaeffler diagram of the AISI 304L plate and AISI 347 bar material is predicting a small amount of martensite. Smallest amount of α' can be expected from AISI 304L pipe material which is located in the austenitic domain. The Schaeffler diagram also considers the expected presence of delta ferrite, whereby the expected quantity of delta ferrite is almost constant for the investigated products. However, it is worth to emphasize, that the above predictions can only give estimations for the α'-formation because they consider the chemical composition only.

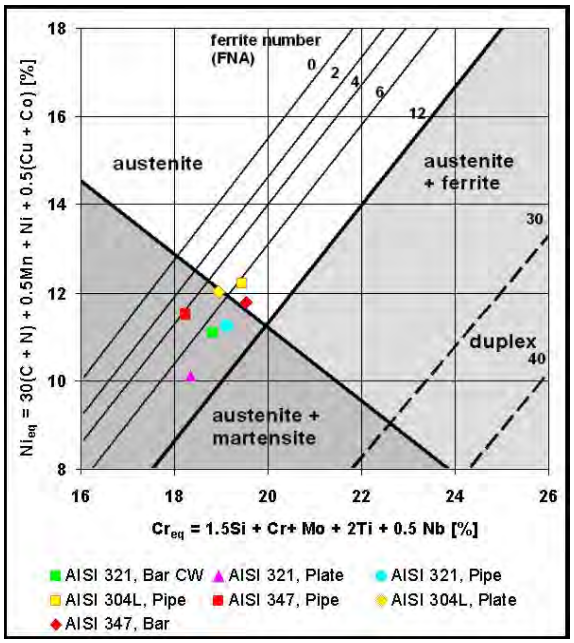

Figure 2: The Schaeffler diagram shows the affinity of the investigated materials for an austenite-martensite phase transition. It shows that AISI 321 and AISI 304L plate material are supposed to have high affinity for martensite formation whereas e.g. AISI 321 pipe and AISI 347 bar and pipe material lying in the austenite regime are not sensitive for α'-trans-formation. In the stabilized grades AISI 321 and AISI 347 the alloying elements C and N are supposed to be fully precipitated as TiCN and NbCN, respectively. Therefore only the remaining fractions of Ti or Nb in solid solution are considered in the Cr equivalent.

Figure 3 shows the microstructures of the material AISI 321 SA pipe, CW bar and SA plate possessing different affinity for strain-induced martensite formation. In the material AISI 321 SA pipe a small amount of α' is found at grain boundaries of the γ-phase, whereas in the CW bar state α' nucleates at lattice defects of the austenite like slip bands and micro-twins created by prior cold working. Little elongated delta ferrite grains (δ) and titanium carbonitride precipitates were also observed.

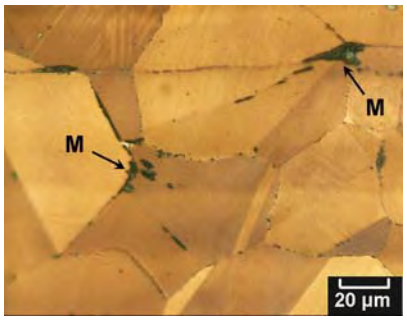

Fig. 3a: AISI 321 SA pipe showing very little martensite (M) at the grain boundaries of the austenitic matrix.

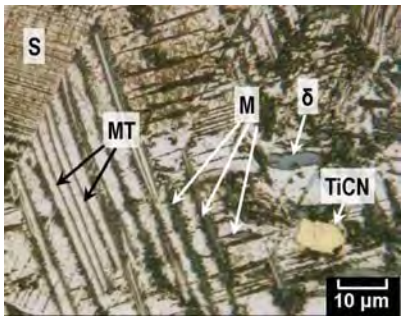

Fig. 3b: AISI 321 CW bar exhibiting lath shaped α' (M) nucleated at lattice defects of the γ, like slip bands (S) and micro-twins (MT) created by prior cold forming process.

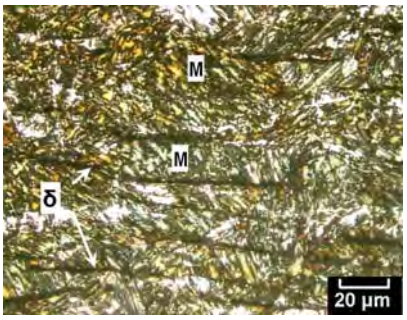

Fig. 3c: AISI 321 SA plate possessing low Cr and Ni content with large regions of dense lath shaped α' (M). Notice the lines of elongated delta ferrite grains (δ).

3. MECHANICAL TESTING CONDITIONS

Fatigue tests were performed at different strain amplitudes and temperatures using a 250 kN closed-loop servo-hydraulic test system of Schenck (Germany) together with the digital Fast Track 8800 controller unit of the Instron Corporation (USA). The strain-controlled low-cycle fatigue tests were performed according to ASTM Standard E606. A climatic chamber of type Instron SFL EC65 (UK) and a high temperature extensometer of type EXA 20-1.25 HT from Sandner Measuring Technique (Germany) were applied. Grips, climatic chamber and extensometer were specially designed for ensuring a short fix length and good axial alignment. To keep the specimen temperature constant, the surface temperature was continuously measured and the air temperature was controlled.

Cyclic load was applied in a sinusoidal waveform with a constant frequency of 0.5 Hz and strain amplitudes of 0.4% or 0.3%, respectively. The fatigue lifetime was defined as the cycles corresponding to a 5% drop in the

maximum stress amplitude. The specimens were fatigued up to different usage factors by varying the cycle number. The usage factor D was defined as the ratio of the applied cycle number to an averaged cycle number representing the technical crack initiation. This averaged value for defining the technical crack initiation was obtained in pre-testing on 3-5 specimens for each testing condition. Hysteresis loops were plotted periodically throughout the fatigue test and the plastic strain and stress amplitudes were determined.

4. DETERMINATION OF MARTENSITIC CONTENT

4.1 Neutron Diffraction Technique

During fatigue the microstructure of the material is changed and some amount of strain-induced martensite is formed in meta-stable austenitic stainless steels. Since the lattice constants of austenite (γ) (a=0.3597 nm) and martensite (α') (a=0.2876 nm) differ, the two phases can be distinguished in scattering experiments by measuring the scattering angle and applying Bragg's law. The contents of the two phases can be calculated from the integrated intensities of the fitted Bragg peaks due to [6].

Since neutrons have a relatively large penetration depth in the material compared with X-rays (in the order of cm instead of μm) information from the bulk are accessible and neutron diffraction (ND) is the appropriate tool for such investigations.

ND experiments with cold neutrons were performed using the powder diffractometer DMC at the PSI neutron spallation source SINQ. This diffractometer is optimised for high intensities that allows to measure martensitic contents below 1 vol-%. The wavelength of the cold neutrons was λ=0.38 nm and the measurements covered a scattering angle of $68° \leq 2\Theta \leq 147°$.

The specimens were fixed on a round table in a vertically position and rotated during the experiment in order to get averaged results. The cross section (gauge volume) of the neutron beam was 20 mm high and 10 mm wide in order to cover the interesting part of the fatigue specimen. This experimental set-up yields an averaged martensitic content over the whole test volume. These averaged values are acceptable because in former experiments a homogeneous distribution of α' in axial direction was observed as long as no cracks are present.

For the body centred cubic (bcc) martensite the 110-reflex and for the face centred cubic (fcc) austenite the 111-reflex, respectively, was investigated. The measured rocking curves shown below were fitted with Gauss functions. For the 111-austenite reflex a scattering angle 2Θ of 132.4° was observed, that corresponds to a lattice constant of a = 3.597 Å for AISI 321 (for pure γ-Fe a value of a=3.60 and for AISI 304L a=3.5911 was found in the literature [5]. However, for high-alloy steel deviations from this value can be expected). The 110-martensite reflex was found at 2Θ =138.20°, that corresponds to a lattice constant of a = 2.876 Å .

To determine the contents of the two phases the scattered neutrons are counted by the detector as a function of the scattering angle. These resulting intensity distributions with peaks at the angles, which correspond to the distance of lattice planes, serve for the determination of the volumetric fraction of phases. Figure 4 shows the Bragg peak for a specimen with 5% martensitic contents, whereas in Figure 5 a large Bragg peak corresponding to about 78% martensite is shown. In addition a ε-martensite peak appeared at 2Θ=120° in the cold worked bar and plate material of AISI 321 grade at temperatures below 0°C. The ε-martensite having a hexagonal close-packed (hcp) lattice, is formed by modifying the stacking sequence of the diagonal 111-planes of the γ-fcc phase. This paramagnetic intermediate phase of ε-martensite may also transform into α'.

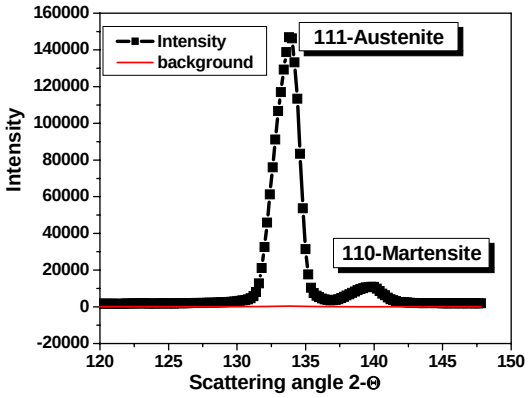

Fig. 4: Neutron intensity spectrum for an AISI 321 bar specimen with 5% martensitic content after 4040 strain cycles of amplitude 0.4% at 80°C.

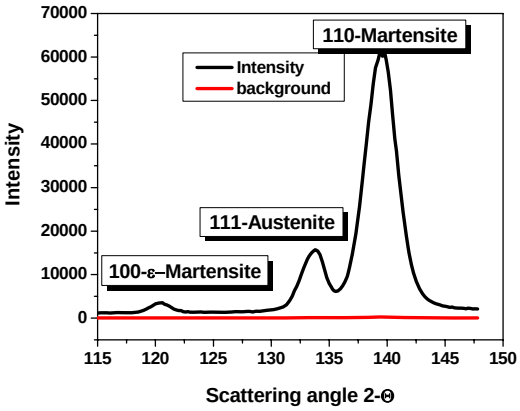

Fig. 5: Neutron intensity spectrum for an AISI 321 plate specimen with 78% martensitic content and an additional ε-martensite peak after 75'000 load cycles with a strain amplitude of 0.3% at -40°C.

4.2 Martensitic contents found by neutron diffraction in different material states

The ND experiments have shown different affinities for the formation of strain-induced martensite. Especially, large differences in the amount of martensite were measured. Whereas in some material a large portion (up to 55% for room temperature) of austenite transformed into martensite, it was less than 0.4% in other material. However, in all measured materials a monotonic increase of martensite versus the number of cycles (noc) was observed.

Fig. 6 shows the martensite content vs. noc for AISI 347 bar which formed a vanishing small volume fraction of α'. For comparison we show in Fig. 7 the result for two sets of AISI 321 bar material which formed about 12% of α'. However, in both cases we observed a linear dependence between the content of α' and the corresponding number of cycles.

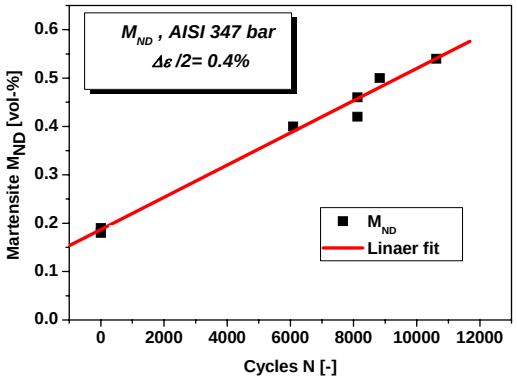

Fig. 6: Volume fraction of martensite vs. cycles for AISI 347 bar. The change of the α'-concentration is very small but shows a linear dependence on the number of cycles.

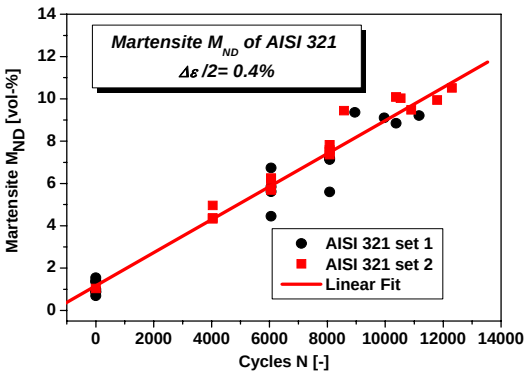

Fig. 7: Volume fraction of martensite vs. cycles for AISI 321 bar. A significant α'-formation can be observed in the cold worked material.

Fig. 8 summarizes the results of the ND-measurements for the materials listed in Tab 2. The strain load amplitude in the fatigue tests was either Δε/2=0.4% or Δε/2=0.3%. The formed martensite is shown up to a number of cycles (noc) where first cracks appeared (corresponding to usage factor D=1). For most materials the dependence of α' on the noc was linear, only in the AISI 321 plate material we observed an exponential growth of α'.

The AISI 321 plate material was very sensitive to the effect of the strain-induced martensite. Thus the measured volume fraction of α' was surprisingly large. Fatigue experiments especially with very small number of cycles confirmed that, -for the described material and loading conditions-, the martensitic content continuously increases during the fatigue life. The martensite formation starts with the very first cycles (Δε/2=0.30%, RT). With increasing noc the martensite growth gets smaller. Furthermore, no threshold for the onset of α'-formation was found for the number of cycles.
The AISI 321 bar formed about 12% α' during cycling with Δε/2=0.40%. However, as shown for the specimens of the same material but machined out from a pipe, only a very small α' growth of about 0.5% was observed.

In AISI 347, the Nb-stabilized material, a small change of α'-content was measured for both, the bar ($0.2\%<M_{ND}<0.5\%$) and the pipe material (<1%).

For AISI 304L a large difference between the cold worked plate (CW), the solution annealed plate (SA) and the pipe material was observed. Whereas the CW material contained between 2% and 5% of α', it was only 0.6% in the SA one, in both cases Δε/2 was 0.4%. In the specimens made out of pipes the α'-phase changed from 0.3% up to 0.7% during 45'000 cycles with Δε/2=0.3%.

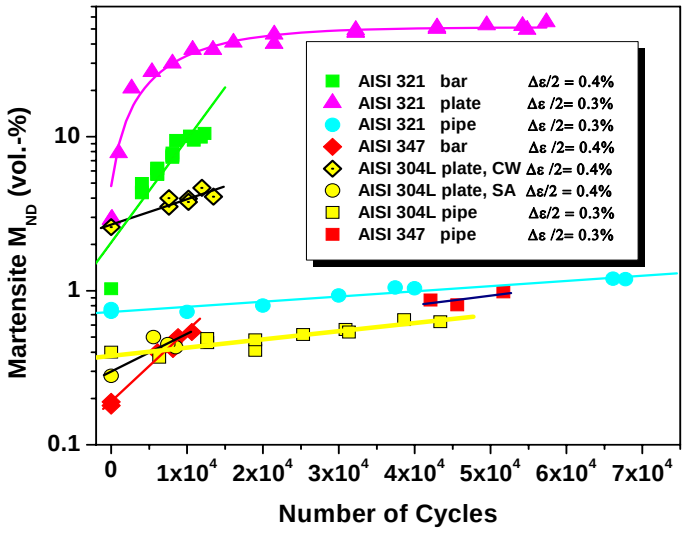

Figure 8: Volume fraction of martensite vs. the number of cycles for all investigated material conditions (neutron diffraction). Varying material conditions result in very different volume fraction of martensite.

It can be summarized that all LCF specimens made from NPP-pipes showed a small affinity for strain-induced formation of martensite. Large amount of α', however, was found in the AISI 321 bar and plate material.

The amount of α' determined by neutron diffraction experiments was used for the calibration of the magnetic methods. We notice that the values of the α'-concentration is always an averaged value taken from a gauge volume. In our experiments this gauge volume was chosen to form the cylindrical part of the fatigue specimens. However, a certain lateral resolution can be achieved within some limits by reducing the size of the incident neutron beam, i.e. decreasing the gauge volume. Since the accuracy of the measured martensite depends on the gauge volume, the intensity of the incident neutron beam and the measuring time, the experiments become very time consuming if highly precise results are to be achieved. We therefore accepted a standard deviation of approximately 0.2%.

5. MAGNETIC MEASURING METHODS

5.1 Ferromaster® for Measuring the Magnetic Permeability

While austenite is paramagnetic, the strain-induced martensite is ferromagnetic. Therefore, if martensite is formed, fatigue also influences the magnetic properties which can be characterized with several parameters.

Among the magnetic parameters which are influenced by fatigue and the corresponding micro-structural changes is the susceptibility (χ_m) or the permeability $\mu_0=1+\chi_m$. In order to investigate the correlation between martensitic content, magnetic susceptibility, usage factor D and other parameters, we determined χ_m by means of an instrument called Ferromaster® (®Product of Stefan Mayer GmbH, Germany). The instrument consists of a ball-shaped permanent magnet to partially magnetize the specimen and two pick-up coils which act as Fluxgate sensors for measuring the resulting magnetic field caused by the volume fraction of α'. If the sensor is contacted

with a fatigue specimen containing α', the magnetostatic field becomes distorted. The degree of distortion measured by the radial component of the magnetic field depends on the martensite content. It is adjusted to yield the susceptibility in a range from 0.0000 to 1.0000 using special reference specimens. The measured permeability can be read from a display. This hand-held instrument is easy to use and its price is moderate.
In contrast to other instruments, the application of the Ferromaster does not need any special surface preparation, neither a preceding magnetization. The relatively large penetration depth of about 1 cm allows of yielding bulk values, which in our fatigue specimens can be compared with the results from neutron diffraction experiments.

5.2 Giant Magneto Resistant Sensor for Measuring of Eddy Current Impedance

The phenomenon of Giant Magneto Resistance (GMR) was discovered 1988 by A. Fert et al. at the University of Paris. This phenomenon appears in thin anisotropic multi-layers made from ferromagnetic and antiferromagnetic materials. A magnetic field applied to such structures results in a giant change of the electrical resistance. The effect is not yet fully understood and is still a topic of research. However, GMR sensors have high importance for technical applications e.g. in digital data storage devices. Detailed literature can be found e.g. in [7].

In our investigations we used a GMR from Non-Volatile Electronics Inc., USA (NVE), which is characterized by a high sensitivity and dynamics, relatively low temperature sensitivity and small size. In our experiments, we applied the GNR in an eddy current (EC) mode, i.e. a magnetic alternating field was applied to the test specimen by a U-shaped magnet, in order to induce eddy currents. These eddy currents are accompanied by a magnetic field with an opposite direction to the incident field. The GMR measures the resulting magnetic field at the surface of the specimen. A special EC-electronics yields the frequency dependent impedance on the base of incident current and GMR-signal. The measuring system allows four different, simultaneous excitation frequencies.

The main parameters influencing the EC-impedance are the frequency f, the electrical conductivity σ and the magnetic permeability μ_r, whereas σ und μ_r are dependent on several micro-structural material parameters [8].

In order to perform scans on the specimen surface a special computer controlled 4-axis (x-, y-, z-translation and one rotation axis) manipulator was built by the Fraunhofer Institut for Non-Destructive Testing, Saarbrücken, Germany. The GMR is guided by a flexible support within an accurate distance over the specimen surface. Since the results of such measurements are very sensitive on the distance of the GMR from the surface (large lift-off effect) special requirements concerning the surface quality have to be fulfilled.

The results of the measurements can be monitored online on the computer screen. Figure 9 a shows representative map from the cylindrical parts of specimens with 8.6% martensite, whereas Fig. 10 shows the result for a specimen with small α' concentration of about 0.5%. Locations where a higher concentration of α' appears may be potential sites for crack initiation.

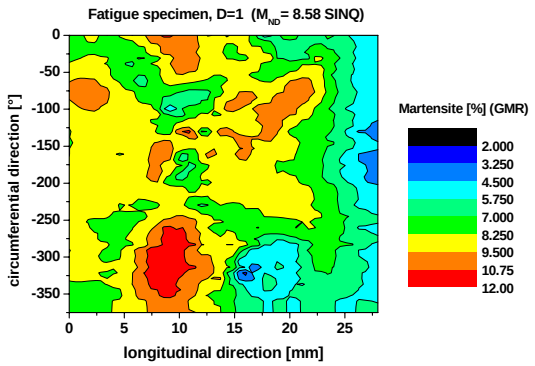

Fig. 9: Distribution of martensite in a fatigued state (D=1). Local maxima martensitic contents of 12% were measured whereas the average content was about 8.6%

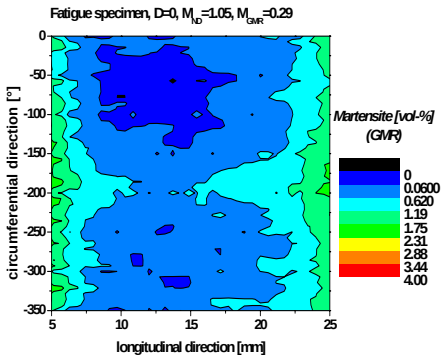

Fig. 10: Distribution of martensite in the un-fatigued state (D=0). The small amount of martensite is rather homogeneous distributed.

5.3 Remanence field measurement by means of 3-D-Fluxgate

An other method to gather information about ferromagnetic precipitations (e.g. martensite) in a paramagnetic austenitic material is the measuring of its magnetic remanence fields. For this purpose we magnetized the specimens up to its saturation, before the remaining field was measured. The magnetisation field of 110 A/m was produced with a specific magnetisation coil. Size and shape of the remanence field yield information about the amount of α' and its distribution. If the distribution of martensite would be known, the corresponding stray field could be calculated based on the following dipole approximation.

$$\vec{B}(\vec{r}) = \frac{\mu_0}{4\pi}\int_{vol}\left\{\frac{3\vec{M}(\vec{r}')\cdot(\vec{r}-\vec{r}')}{|\vec{r}-\vec{r}'|^5}(\vec{r}-\vec{r}') - \frac{\vec{M}(\vec{r}')}{|\vec{r}-\vec{r}'|^3}\right\}d^3r' \qquad \text{(Eq. 3)}$$

This means, the magnetic field vector B(r) could be calculated at each point r. M(r') is the concentration of magnetic dipoles (corresponding to the concentration of α'), r and r' are position vectors pointing from the origin to measuring point of M and the location of the magnetic dipoles, respectively; μ_0 is the magnetic field constant. Since the integration in Eq. 3 ranges over the whole volume of the specimen the reverse magnetic problem, i.e. the determination of M(r'), is not isomorphic. This makes the quantitative determination of α' and its location very difficult. However, for some simple cases the localisation of inhomogeneous martensite distribution is feasible.

The equipment for remanence field measurement consists of high sensitive magnetic field sensors, a control unit, a data acquisition device and a manipulator system. For our measurements a 3-axis Fluxgate of type FL3-100 from Stefan Mayer GmbH (Germany) was applied.

The excellent sensitivity of the Fluxgate sensor allows measuring of magnetic fields in the nT range. However, the fields created by martensitic contents usually are below 1 μT and ambient fields can be much larger, e.g. the earth magnetic field is in the order of 40 μT. This makes measurements in un-shielded environments very difficult. Therefore our fatigue specimens were measured in a special chamber shielded with a material of high permeability.

In order to measure the remanence field, the specimen was moved in x- and y-direction for performing scans. The remanence field was scanned either on a plane or on a line at a certain distance from the specimen. In our measurements this distance was 110 mm. The increase of the martensite content results in higher values of the remaining magnetic induction (remanence).

5.4 Results from magnetic measurements

After calibrating the magnetic sensor system by means of specimens with a known amount of martensite, the contents of martensite were determined by the magnetic methods described above. All these methods allowed the detection of strain-induced martensite in the investigated austenitic stainless steels in laboratory environment. Even for very small concentrations of martensite it was possible to observe a clear correlation between the number of cycles and the corresponding magnetic properties. Figures 11-12 show the ferromagnetic contents as a function of the noc determined by the 3 magnetic methods. For comparison also the α'-concentration M_{ND} measured by neutron diffraction is shown in the same figures. The M_{ND} observed on a subset of specimens was used to calibrate the magnetic devices.

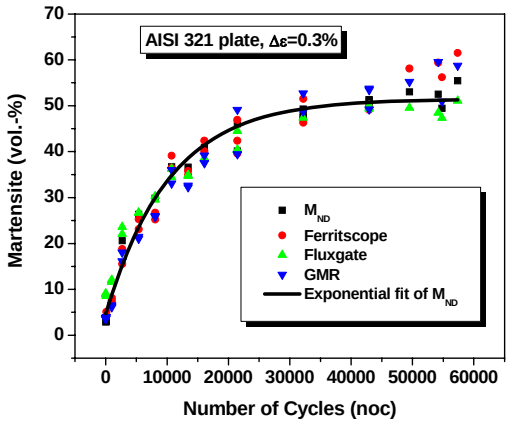

Figure 11: Volume fraction of martensite vs. fatigue life for the AISI 321 plate material. The magnetic methods are compared with the results from neutron diffraction.

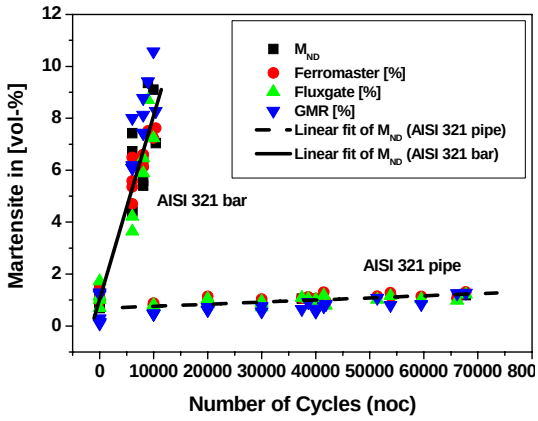

Figure 12: Volume fraction of martensite vs. fatigue life for the AISI 321 pipe and bar material, evaluated by ND and magnetic methods.

As shown in the above figures, good agreement between the martensitic contents evaluated with magnetic methods and those obtained by neutron diffraction was found. The scatter observed in the figures is manly caused by inhomogeneities in the material properties. For very low martensitic concentrations as it appeared in the AISI 321 pipe or AISI 347 bar material the noise to signal ratio is too large for a reliable prediction of fatigue life.

Differences between the results obtained by neutron diffraction and magnetic methods can be observed for number of cycles where cracks appear (N_f). The reason for this difference is that martensitic contents measured by ND are averaged over the bulk (gauge volume), whereas some magnetic methods are more sensitive to local martensite concentrations.

6. Influence of operation temperature on martensite formation

Beside strain amplitude, cycle number and some material properties (chemical composition, heat treatment) the test temperature played an important role for the effect of strain-induced martensite. Therefore, low-cycle fatigue tests were performed for the different material states of AISI 321 at various temperatures. In the Figs. 13-16 the volume fraction of α' as a function of the test temperature is specified for every material state in detail.

For lifetime assessment models based on the strain-induced martensite, it is necessary to investigate the martensite formation in a wide temperature range. In Fig. 13 the temperature dependence of the α' formation in a temperature range from -100 °C up to 260 °C is shown. The results of the neutron diffraction experiments for the bar and plate materials are shown. The α'-content vs. temperature curves showed a typical S-shape. A similar temperature behaviour of the strain-induced α' was observed for quasi-static loading [9]. At temperatures below -50 °C, the austenitic stainless steel is almost completely transformed into a martensite structure. In the temperature range of $-50\ ^{o}C \le T \le 100\ ^{o}C$, the martensite content for the plate and bar materials is strong dependent on the temperature. If the susceptibility to the α' transformation increases (bar to plate material) the α'-content vs. temperature curve is shifted towards higher temperatures. The temperature dependence of the martensitic transformation was described by the Boltzmann function

$$c_{\alpha'} = (c_{\alpha'})_o + A/\{1+\exp[(T-T_o)/B]\} \quad , \qquad \text{(Eq. 5)}$$

in which $c_{\alpha'}$ and $(c_{\alpha'})_o$ are martensite contents for the fatigued and the initial material state. A, B, and T_o are fitting parameters.

The temperature dependence of the α' formation in the plate material is specified in Fig. 14. Results of the Ferromaster, Fluxgate and GMR magnetic methods are presented in the same figure. With respect to the application of the method the temperature range was limited to $60\ ^{o}C \le T \le 260\ ^{o}C$. Above 150°C only a small change of the martensitic content was measured.

Fig. 15 shows the influence of the test temperature on the α'-content in the AISI 321 bar material from room temperature up to 260 °C. The volume fraction of α' for this material continuously decreases with increasing

temperature. In the investigated temperature range, the best-fit curve was described by an exponential decay function.

$$c_{\alpha'} = (c_{\alpha'})_o + A\exp[-(T - T_o)/B] \qquad \text{(Eq. 6)}$$

In Fig. 16 the temperature dependent curve for the α' formation of the AISI 321 pipe material is shown. For temperatures higher than room temperature the martensite content was about the same than for the as-received condition. Therefore it was concluded that this pipe material was not susceptible to the formation of fatigue-induced α' under the given loading and temperature conditions. For room temperature a small increase of the volume fraction of α' was observed. For the AISI 321 pipe material it thus is very difficult to perform lifetime assessment using the effect of fatigue-induced α'.

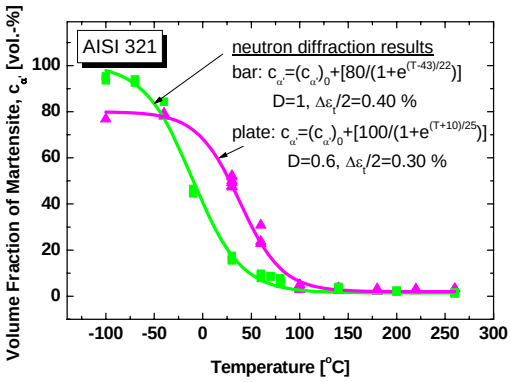

Figure 13: Fatigue-induced martensite content vs. temperature for the AISI 321 plate and bar materials (neutron diffraction).

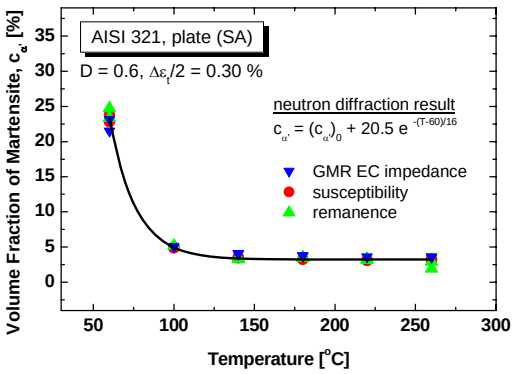

Figure 14: Fatigue-induced martensite content vs. temperature for the AISI 321 bar material (magnetic measurements).

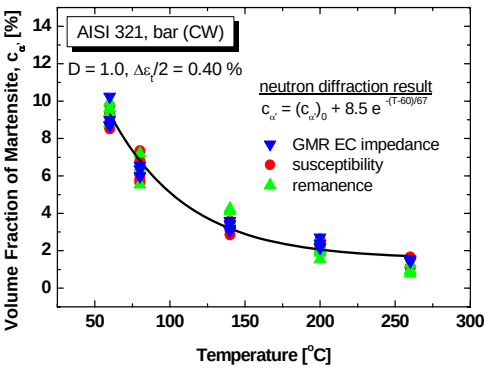

Figure 15: Fatigue-induced martensite content vs. temperature for the AISI 321 plate material (magnetic measurements).

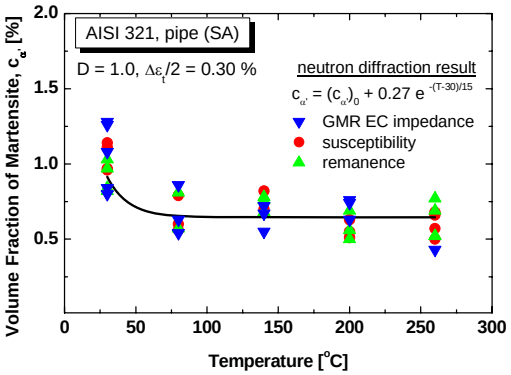

Figure 16: Martensite content vs. temperature for the AISI 321 pipe material (magnetic measurements).

7. EFFECT OF THE STRAIN AMPLITUDE

For the piping material AISI 321 strain-controlled fatigue experiments were performed at different strain amplitudes. After fatigue the volume fraction of martensite was measured by means of the different magnetic methods. Results are shown in Fig. 17. For all levels of the strain amplitude a monotonic increase of the martensite content with rising numbers of cycles was observed. The effect of the strain-induced martensite formation was higher for low values of the strain amplitude but large cycle number and the corresponding large accumu-

lated plastic strain. For the given material conditions there is an opportunity to apply the method for early detection of fatigue damage in cases where strain amplitudes are low and cycle numbers are high.

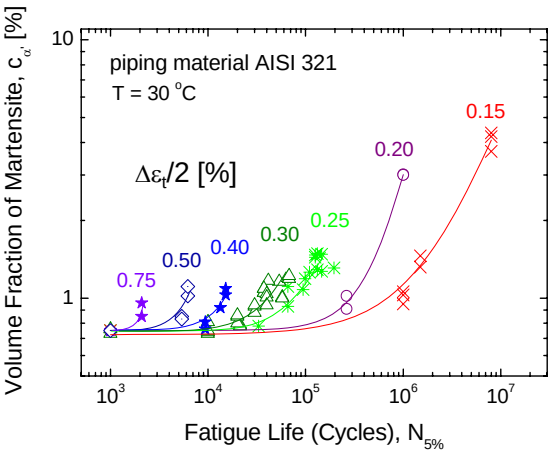

Figure 17: Volume fraction of martensite vs. fatigue life obtained for different strain amplitudes.
Small strain amplitude resulting in higher amount of martensite at end-of-life.

8. RANKING OF MAGNETIC METHODS

8.1 Quality, Applicability and Costs

The objective of this chapter is to analyse the NDT results quantitatively in terms of their accuracy, reproducibility and scatter of results versus material degradation parameters, and to compare the performance of the different magnetic NDT techniques. However, a fair comparison of the magnetic methods is difficult at present state because the methods are in different development states, they might yield different or complementary information about the material and can depend on the problem to be analysed. Further, the application in a laboratory environment differs from that in a real industrial one.

However, Tab. 7 summarizes the ranking results obtained with the magnetic methods. The ranking is based on the laboratory experiments with a special set of fatigue specimens. In this ranking we tried to include as well practical and economical aspects which cannot be exactly quantified, beside of the measurable quantities. The results of the analysis are based on:

- **Quality of the measured values** is based on repeatability of measurements on a selected set of specimens. (Standard deviation (SD) referred to the measuring range). The functional relationship between measuring value and required quantities, given by the correlation coefficient and standard deviation, evaluated by a simple one-dimensional analysis. In order to quantify the repeatability of measurements we calculated the standard deviation from 10 repeated measurements of three selected specimens made from AISI 321 bar material (PN01: M_{ND}=10%, PN10: M_{ND}=5.6%, PN15: M_{ND}=1%) containing different amount of martensite (M_{ND}). Such measurements cannot include all the influencing parameters, but might yield a measure for the uncertainty of the method. In Tab 7 only the averaged SD from the three sets is given for each of the applied NDT-methods. Since the results shown in Tab. 7 stem from repeatability tests performed in one measuring session (short time between the measurements) they are rather good.

- **On-site applicability** based on the handling of device and technique for performing the measurements, complexity of device handling and installation methods and on special requirements of component and local environment (access, surface finish, temperature, humidity, etc.). Further on durability / service life of device in site environment, possible modes of operation (on line measurement, periodic measurement during outages, tests on components in-situ), time required for measurements, feasibility of transferring device/technique from laboratory to site environment (temperature, humidity, vibration, difficult access, etc).

- **Costs of NDT-technique,** including future development, training of technicians and maintenance costs.

8.2 Correlation Between Measured Results and Required Quantities

The correlation coefficient is the measure for the functional relation between measuring values and required quantities. These quantities are for LCF-specimens the number of cycles and the martensite content, respectively.

For the interpretation of the results it is important to stress that the SD given in Tab. 7 is the SD in % of the full range taken from the linear fit of the analysed data. Therefore they include the scatter of the martensitic content, which is already present due to material inhomogeneities and differences in the fatigue process. This means that the SD given in Tab. 7 is a measure of the quality of the method as an application and does not reflect the quality of the measuring system alone. Since in some material grades the scatter in the martensitic content obtained is relatively large, especially if only a few martensite was formed, the relative SD in % of the measuring range is rather large and the correlation coefficient might be small.

The score for the correlation coefficient is based on the values given for the different specimen sets (Tab. 7). All methods got high score based on the repeatability tests, which were performed in one measuring session with the same calibration. However, from other measurements not documented in this report, we know that the repeatability has to be judged carefully. If measurements have to be repeated several weeks later, new calibration may be necessary and results could look different.

In general, best scores were reached with Ferromaster, followed by GMR. Fluxgate sensors got lower score due to practical aspects. Such measurements have to be performed in a magnetically shielded environment. However, in laboratory environment their performance is comparable to the other methods.

Tab. 7: Ranking of magnetic NDT-methods applied at PSI

	Score	Ferromaster	GMR	Fluxgate
Quality of measured values	Correlation between measured value and number of cycles	0.9	0.9	0.95
	Standard deviation in % Scatter from repeatability tests	0.354	0.35	2.3
Applicability	Handling	Very easy	easy	easy
	Applicability	easy	difficult	test specimens
	Durability	good	medium	good
	Measuring time	fast	fast	fast
	Preparation of specimen	no	surface	magnetization
	General judgement	**recommended**	**promising**	**Laboratory only**

9. DISCUSSION

9.1 Neutron diffraction

The results obtained from ND allow some conclusions concerning the influencing parameters for strain-induced formation of martensite:

The highest martensitic content was formed in the AISI 321 plate material where maximum values up to 56% were measured. Very low martensitic content ranging from 0.2 to 0.6% was found in specimens made from AISI-347 bar material. However, even for such low concentration of α', a clear increase with the number of cycles was observed. Lowest changes of the α'-concentration during the fatigue test were measured in all the pipe materials.

In AISI-304L martensitic contents of about 3% for the cold-worked and about 0.5% for the solution annealed state was found. A very small rise of martensitic content vs. the noc was observed in this material. The comparison of these two different material states shows the influence of the cold working. This result is in agreement with the same observation made in the AISI 321.

For all material conditions the volume fraction of α' is dependent on the test temperature. The temperature dependence of the martensite formation was described by an exponential decay function in the temperature range relevant for the nuclear power plant operation. For the plate and bar materials the martensite vs. temperature curve has to be considered for lifetime assessment. In case of the AISI 321 pipe material the amount of fatigue-induced α' is low at temperatures higher than room temperature.

It was shown that the Schaeffler diagram is able to qualitatively assess the amount of the fatigue-induced α' for the solution-annealed material. As farer the material is located in the two-phase region austenite + martensite, mainly due to lower Cr and Ni content, the more strain-induced martensite is formed. Therefore, the pipe and plate material AISI 304L and the bar material AISI 347 possess the highest austenite stability, the plate material AISI 321 the lowest. This result was confirmed by the results from ND.

The final heat treatment of the steel had also an influence on the martensite formation during fatigue. The lattice defects like slip bands or micro-twins due to the cold-drawing process act as nuclei for the transformation

of austenite to α'. The solution-annealed material does not have such defects, and fatigue creates only little of them. In the case of the cold-worked material an accelerated martensite formation was observed in comparison with the pipe material. As shown in [9] the yield strength can be used to assess the degree of the cold working.

The influence of the actual chemical composition and the final heat treatment on the martensite formation in austenitic stainless steels has some consequences for the technical application of the method. Prior to its application, information about the chemical composition and the yield strength is necessary to assess the susceptibility of the given stainless steel to the formation of strain-induced α'. If the effect of the martensite formation is assessed to be high enough, the calibration curves of the fatigue-induced martensite for different strain amplitudes and temperatures can be obtained in laboratory testing.

9.2 Magnetic methods

All the applied magnetic methods allowed the detection of strain-induced martensite in the investigated austenitic steels. A linear relation between the volume fraction of martensite and the magnetic properties was found. This, in principle, allows the usage factor or the remaining lifetime of a specimen to be determined by non-destructive magnetic measurements. However, the application of some magnetic methods to real components is limited due to practical aspects. Thus, differences between the methods are mainly found in the applicability of the various methods.

Measuring the magnetic susceptibility using the Ferromaster device is the easiest and cheapest method that yields a very strong (linear) correlation between permeability and martensitic content. Susceptibilities from 0.04 up to 0.28 in fatigue specimens were measured. The measuring range of the Ferromaster $0<\chi_m<1$, corresponding to a ferromagnetic content of about 0-20% was sufficient to cover the susceptibilities in most specimens except for the AISI 321 plate material. For the latter an instrument named Ferritscope from Fischer company was used to estimate the amount of martensite. No special conditions have to be fulfilled concerning the surface of the specimen. With this method the gauge volume is relatively large and the penetration depth is more than 10 mm. Compared with the size of our fatigue specimens, the size of the sensor head is large and the consequence is an influence of the specimen/component geometry. This is not a serious disadvantage and can be corrected by an appropriate calibration. As shown in [10], the Ferromaster can also be used for in-situ monitoring. We therefore recommend the application of the Ferromaster for NDT of in-service components.

Remanence field measurements using Fluxgate magnetometers are very sensitive and give precise and reproducible results. A disadvantage of this method is that the specimen under investigation has to be magnetised in advance up to a defined level. For low ferromagnetic content the remanence field is very small (some tens of a μT to a few μT) and in an un-shielded environment the background fields for such measurements are too large. For this reason the method is restricted to basic studies in the shielded laboratory.

GMR sensors can be used as to measure the EC-impedance. The high sensitivity of these sensors and the fact that they can be used in an unshielded environment are the reasons for the promising potential of this method. A disadvantage is the high sensitivity on the distance between sensor and surface of the specimen (lift-off-effect). The method is also very sensitive to other influencing parameters, e.g. material type and temperature. Therefore these parameters have to be included in the calibration or must be held constant during measurements. This method is not limited to austenitic steels and we believe that it has a potential for various NDT-applications.

10. CONCLUSIONS

In this paper we discussed the application of magnetic NDT-methods for lifetime prediction of low cycled austenitic stainless steel, namely the determination of magnetic permeability, measuring the eddy current impedance and the remanence field measurement. The methods mentioned above were calibrated using martensitic contents measured by neutron diffraction.

From the magnetic methods, especially measuring the magnetic permeability with the Ferromaster can be recommended for the application to NDT. Also measuring the EC-impedance with GMR-sensors is very promising and might not be limited to austenitic steels. Remanence field measurement is a very precise method as long performed in shielded environment but is limited to the laboratory since disturbing ambient noise is to large compared with the small field resulting from the component.

Various austenitic stainless steel with different low cycle fatigue load and processing histories were analysed concerning their affinity for strain-induced martensite formation. Large differences in the martensitic contents between the investigated specimen sets were found. We therefore conclude that the amount of martensite alone is not a sufficient general criterion for end of life prediction, since the chemical composition of the material, its initial degree of cold working and the operating conditions (e.g. temperature, mechanical loading) have significant influence on the martensite formation. Thus, these parameters have to be taken into account for the application of the described magnetic NDT-methods. However, for specific testing conditions good correlation between

the formed amount of martensite and the number of fatigue cycles was found. Therefore, material and operating specific calibration curves have to be evaluated in order to allow reliable lifetime predictions of real components.

The results presented in this paper can contribute to failure analyses of austenitic stainless steel components. For safety relevant components made from meta-stable austenitic steel, an increase of the martensitic phase content is an indication for a certain accumulated plastic deformation. A screening criterion for the volume fraction of martensite for the given material and loading condition can be used to avoid damage of components due to thermo-mechanical fatigue.

11. ACKNOWLEDGMENTS

We are grateful to the "Federal Office for Education and Science", the "Swiss Federal Nuclear Safety Inspectorate (HSK)" and the "Swiss Federal Office of Energy (BFE)" for their financial support of the research.

Thanks are also expressed to Mr. E. Groth and Mr. M. Stricker for performing of the fatigue tests and the magnetic measurements. The neutron diffraction experiments were performed at the SINQ, Paul Scherrer Institut, Switzerland. We would like to thank Dr. L. Keller for his kind assistance at the DMC of the SINQ.

12. REFERENCES

1 Niffenegger M., Grosse M., Kalkhof D., Leber H. (PSI), Vincent A., Pasco L., Morin M. (INSA de Lyon), "Material Characterization of Fatigue Specimens made from Meta-stable Austenitic Stainless Steel", 2003, PSI Report No. 03-17.

2 Kalkhof D., Grosse M., Niffenegger M. and Leber H. J., "Fatig Fract Mater Struct",2004, Vol. 27 595–607.

3 Angel, T., "Formation of Martensite in Austenitic Stainless Steels", J. Iron and Steel Institute, 1954, Vol. 177, 165-175.

4 Leber H.J., Kalkhof D., Niffenegger M.,"Effect of metallurgy and heat treatment on strain induced martensite formation in low cycle fatigue austenitic stainless steel", 7th International Conference on Engineering Structural Integrity Assessment, Manchester, UK, 2004.

5 JCPDS-International Centre for Diffraction Data, 2001.

6 Bacon G.E., "Neutron Diffraction", Clarendon Press, Oxford, 1975.

7 Grünberg P., "Riesenmagnetowiderstand in magnetischen Schichtstrukturen", Physikalische Blätter 51, 1995, 1077-1081.

8 Becker R., "Über die Prüfung auf Fehler in metallischen Werkstoffen und Bauteilen mittels eines zerstörungsfreien Mehrfrequenz-Wirbelstrom Prüfverfahrens", Diss. Uni. des Saarlandes, 1980.

9 Kalkhof D., Leber H.J., Niffenegger M., "Fatigue-induced martensite in different qualities of the austenitic stainless steel AISI 321",3th International Conference on Fatigue of Reactor Components, Sevilla, Spain, 2004.

10 Niffenegger M., Bauer R., Kalkhof D., "Non-destructive determination of martensitic content by means of magnetic methods", PSI-Report no. 03-19, ISSN 1019-0643, 2003.

